DOI: 10.1002/ejic.200601040

An Unusual Carbonyl Chemical Shift in a Carbonylhexairidium Cluster: A Combined Solid-State NMR and DFT Approach

Michele R. Chierotti,[a] Luigi Garlaschelli,*[b] Roberto Gobetto,*[a] Carlo Nervi,[a] Giulia Peli,[b] Annalisa Sironi,[b] and Roberto Della Pergola[c]

Keywords: NMR spectroscopy / DFT calculations / Carbonyl cluster / Iridium / Chemical shift tensors / Shielding anisotropy

The ^{13}C NMR spectrum of $TMBA_2[Ir_6(CO)_{15}]$ [TMBA = $(CH_3)_3N(CH_2C_6H_5)$] shows, at low temperatures, an unprecedented μ_2-bridging carbonyl low-frequency shift, with the resonances of the terminal μ_1-carbonyl ligands placed at higher frequencies. The chemical shift tensors and the shielding anisotropies of the carbonyl ligands, obtained from solid-state NMR analysis, allow us to determine the nature of the M–CO interaction. The results have been compared with the ^{13}C MAS data of $Ir_6(CO)_{16}$ where μ_3-CO ligands are present. Further evidence for the assignment and for the peculiar chemical shift value of bridging carbonyl ligands in $TMBA_2[Ir_6(CO)_{15}]$ has been obtained by the DFT calculation of the NMR parameters. The scalar and spin-orbit (SO) relativistic two-component zero-order regular approximation (ZORA) methods were employed in the geometry optimization and NMR chemical shift calculations, respectively. The large SO contribution (δ = 26.6 ppm) to the μ_2-bridging CO ligand ^{13}C chemical shifts accounts for the position of the experimentally observed resonance.

Introduction

Medium- to high-nuclearity carbonylmetal clusters may present terminal, double-bridging (μ_2) and triple-bridging (μ_3) CO ligands. Thanks to the different M–CO bonding order, it is possible to discriminate the three kinds of ligands by means of spectroscopic techniques such as IR and ^{13}C NMR spectroscopy. Increasing the back-bonding in the coordination between metal atom and carbon monoxide ligand results in a higher frequency shift of the CO resonances. Indeed, in most cases CO chemical shifts follow the series:[1] $\delta(M–CO) < \delta(M_2–\mu_2\text{-}CO) < \delta(M_3–\mu_3\text{-}CO)$.

Also within subgroups there is a progressive low-frequency shift as the atomic number increases, for example:[1] $\delta(Co–CO) > \delta(Rh–CO) > \delta(Ir–CO)$.

Stereochemical nonrigidity both in solution and in the solid state is a common feature of carbonylmetal clusters and is well documented in several papers.[2] In many cases, however, solution structures were fully consistent with solid-state X-ray structural determination.

Most carbonyliridium clusters present a complete CO fluxionality at room temperature that yields magnetically equivalent ligands; usually the low-temperature spectrum shows signals between δ = 160 and 180 ppm for terminal CO ligands, between δ = 180 and 210 ppm for the edge-bridging ones and between δ = 220 and 260 ppm for the μ_3-CO ligands.[1]

In this paper we report the NMR characterization of two carbonyliridium clusters, namely $[Ir_6(CO)_{15}]^{2-}$ and $Ir_6(CO)_{16}$. Both compounds have been previously synthesized in 1970 by Malatesta and co-workers,[3] but only in the middle of the 1980s did we manage to determine the cluster's structures. $[Ir_6(CO)_{15}]^{2-}$ shows 12 terminal and three edge-bridging CO ligands,[4] while $Ir_6(CO)_{16}$ has been isolated in two different isomeric forms: a red and a black isomer, the latter being quite unstable.[5]

Our aim is to elucidate and compare the particular spectroscopic properties of the $[Ir_6(CO)_{15}]^{2-}$ and $Ir_6(CO)_{16}$ complexes, using a combined experimental-theoretical approach, employing solid-state NMR and DFT calculations of ^{13}C NMR chemical shifts. Within this paper the discussion of only the red isomer of $Ir_6(CO)_{16}$ has been taken into account.

Results and Discussion

Spectroscopic Results

The compound $Ir_6(CO)_{16}$ is isostructural with $Rh_6(CO)_{16}$, with four face-bridging and 12 terminal carbonyl

[a] Dipartimento di Chimica Inorganica, Chimica Fisica, Chimica dei Materiali, Università degli Studi di Torino,
Via P. Giuria 7, 10125 Torino, Italy
E-Mail: roberto.gobetto@unito.it
[b] Dipartimento di Chimica Inorganica, Metallorganica e Analitica, Università degli Studi di Milano,
Via G. Venezian 21, 20133 Milano, Italy
[c] Dipartimento di Scienze dell'Ambiente e del Territorio dell'Università di Milano-Bicocca,
Piazza della Scienza 1, 20126 Milano, Italy

ligands.[5] However, in solution they show very different behaviors. Indeed, $Rh_6(CO)_{16}$ possesses an O_h symmetry and its spectrum, reported by Heaton et al.,[6] is characterized by two resonances, in a 3:1 ratio, at δ = 180.1 and at 231.5 ppm attributed to the terminal and bridging (μ_3) carbonyl ligands, respectively. On the contrary, the ^{13}C NMR solution spectrum of $Ir_6(^{13}CO)_{16}$ in CD_2Cl_2 displays a single peak at δ = 177.60 ppm clearly indicating the presence of chemical exchange among the carbonyl ligands. Even though we used a ^{13}C-enriched sample, the low solubility of the cluster did not allow us to perform variable-temperature (VT) experiments.

In the solid state $Ir_6(CO)_{16}$ possesses a simple C_2 symmetry. Hence, for this reason we expect two distinct signals for the bridging carbonyl ligands and six overlapped peaks for the 12 terminal ligands as already observed for $Rh_6(CO)_{16}$. Indeed, the carbonyl isotropic region of the solid-state spectrum (Figure 1) is characterized by three peaks at δ = 168.8, 203.9, and 209.2 ppm assigned to the terminal and to the two pairs of equal μ_3-CO ligands, respectively. Because of the overlapping of the signals, instead of six resonances for 12 terminal carbonyl ligands only a single broad asymmetric peak with a shoulder at $\delta \approx$ 166.8 ppm is observed, as has already been seen for the isostructural $Rh_6(CO)_{16}$.[6]

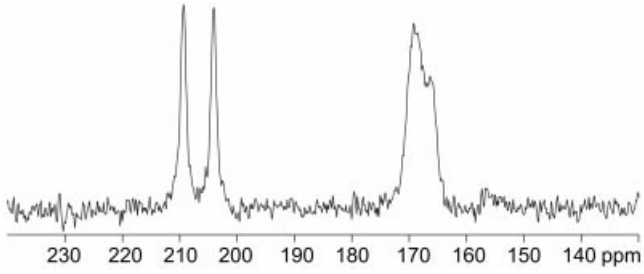

Figure 1. Isotropic region of the solid-state ^{13}C MAS NMR spectrum of $Ir_6(^{13}CO)_{16}$ recorded at 68.7 MHz, 25 °C, and at a spinning speed of 5.9 kHz.

We also performed an analysis of the chemical shift tensors δ_{11}, δ_{22}, δ_{33}, where $\delta_{11} \geq \delta_{22} \geq \delta_{33}$, and of the shielding anisotropy (CSA) of the different carbonyl signals, defined as $\Delta\sigma = \sigma_{33} - (\sigma_{11} + \sigma_{22})/2$ with $\sigma_{11} \leq \sigma_{22} \leq \sigma_{33}$. By recording a spectrum at a low spinning speed (about 3.8 kHz) (Figure 2) it has been possible to calculate the chemical shift tensors by means of the Herzfeld–Berger method.[7] The obtained tensor values, as well as the shielding anisotropy $\Delta\sigma$, are reported in Table 1. Unfortunately, for the μ_3-carbonyl moieties the analysis is slightly approximated due to the small amount of overlapping between the resonances. The terminal CO ligands show a shielding anisotropy value ($\Delta\sigma$ = 385.9 ppm) with pseudo-axial symmetry similar to that observed for the terminal carbonyl ligand of many other organometallic compounds such us $Rh_6(CO)_{16}$, $Os_3(CO)_{12}$, etc., (about 400 ppm).[8] On the other hand, as expected, the bridging (μ_3) carbonyl ligands give rise to a smaller anisotropy of 114.6 ppm. It is worth noting that the chemical shift tensor of the bridging CO sites is axially symmetric due to the threefold rotational symmetry about the C–O axis.

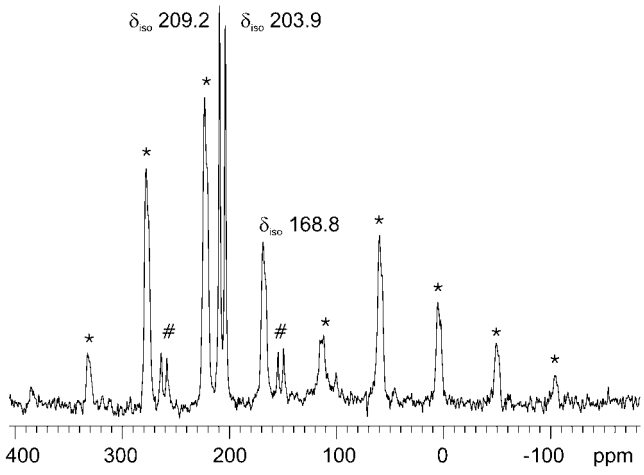

Figure 2. Solid-state ^{13}C MAS NMR spectrum of $Ir_6(^{13}CO)_{16}$ recorded at 68.7 MHz, 25 °C, and at a spinning speed of 3.8 kHz. Spinning sidebands marked with * are associated with the peak at δ = 168.8 ppm, while those marked with # are related to the peaks at δ = 209.2 and 203.9 ppm.

Table 1. ^{13}C chemical shift tensors, shielding anisotropy, and integral values for compound $Ir_6(CO)_{16}$. The shielding anisotropy is defined as $\Delta\sigma = \sigma_{33} - (\sigma_{11} + \sigma_{22})/2$ with $\sigma_{11} \leq \sigma_{22} \leq \sigma_{33}$ and $\delta_{ii} = -\sigma_{ii}$.

δ_{iso} [ppm]	δ_{11} [ppm]	δ_{22} [ppm]	δ_{33} [ppm]	$\Delta\sigma$ [ppm]	Integral value
168.8	352.7	241.9	–88.6	385.9	12
203.9	244.8[a]	244.8[a]	130.3[a]	114.6[a]	4
209.2					

[a] The spinning sideband analysis was performed by considering a single peak, due to high-resonance overlapping. All these resonances are associated to bridging ligands and then a similar anisotropy is expected.

The structure of $[Ir_6(CO)_{15}]^{2-}$ has been previously reported by Demartin et al.[9] Briefly, it consists of a regular octahedron of stereochemically equivalent iridium atoms connected to 12 terminal and three symmetrically edge-bridging (μ_2) carbonyl ligands. The 12 terminal CO ligands can be divided into two sets, six of them being in an axial and six in an equatorial configuration.

The VT ^{13}C NMR experiments of a ^{13}CO-enriched sample of $TMBA_2[Ir_6(^{13}CO)_{15}]$ dissolved in $[D_8]THF$ are reported in Figure 3. In the range 173–298 K the NMR spectroscopic data clearly show the presence of one or more fluxional processes involving the carbonyl resonances. At room temperature the spectrum is characterized by a single peak at δ = 191.9 ppm. By decreasing the temperature, the signal broadens and the coalescence temperature is reached at 213 K. By further decreasing the temperature, it is possible to freeze the fluxionality, and three signals appear at δ = 201.1, 191.2, and 175.2 ppm with relative intensities of 6:6:3, respectively. A careful inspection of the VT spectra reveals that the resonance centered at δ = 201.1 ppm in the

temperature range 203–183 K is sharper than the other two resonances; thus, at least two different processes involving the carbonyl ligands determine the fluxional behavior of $TMBA_2[Ir_6(^{13}CO)_{15}]$. The presence of three resonances in the low-temperature limiting spectrum (173 K) agrees with the X-ray structure in which three different types of carbonyl ligands are present (two sets of six terminal CO ligands and one set of three μ_2-CO ligands).

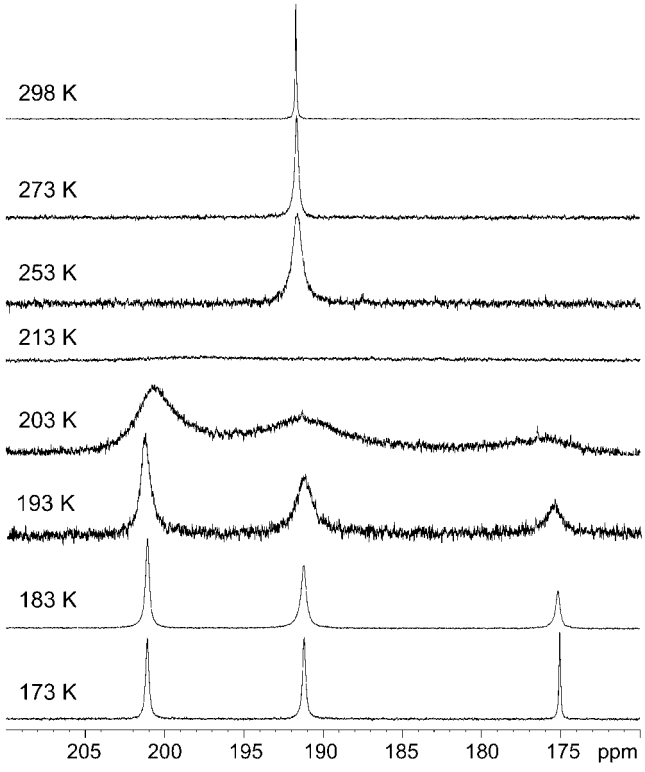

Figure 3. Solution VT ^{13}C NMR spectra of $TMBA_2[Ir_6(^{13}CO)_{15}]$ recorded at 151 MHz in the temperature range 173–298 K.

One would expect the bridging carbonyl signals to fall at a higher frequency with respect to the terminal ones, in this case we need to assume an unprecedented low-frequency value for the bridging CO resonance (δ = 175.2 ppm), and a quite high chemical shift value for the two sets of terminal carbonyl ligands. These results, never reported before, prompted us to find experimental evidence for our assignment. Solid-state NMR is often used as a bridge technique between the solid structure obtained by single crystal X-ray determination and solution NMR spectroscopic data. For this reason we decided to undertake a solid-state NMR investigation of the molecule in order to find NMR parameters corroborating our assignment.

The whole ^{13}C MAS spectrum of $TMBA_2[Ir_6(^{13}CO)_{15}]$ is reported in Figure 4. In the carbonyl isotropic region (Figure 5) it is possible to observe 11 isotropic resonances, at δ = 179.0, 181.5, 184.2, 187.1, 189.5 (sh), 190.5, 193.8, 196.1, 198.3, 202.3, and 205.3 ppm. It is worth noting that the intensities of the signals are quite different and in particular higher integration values are associated with the signals that fall at δ = 179.0, 184.2, and 196.1 ppm. It is well known that the intensities of the isotropic peaks in solid-state NMR spectra cannot be directly compared without considering the different spinning sideband patterns associated with each resonance (see Figure 4). By careful integration of the isotropic and anisotropic part of the spectrum, we can conclude that all the peaks have the same cumulative intensity except the signals at δ = 179.0, 196.1, and 205.3 ppm where the relative intensities are 2:3:2 with respect to the other resonances. Thus, the number and the intensities of the peaks are in agreement with the presence of 15 carbonyl ligands.

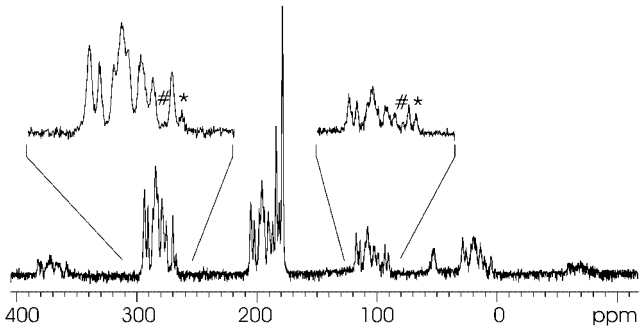

Figure 4. Solid-state ^{13}C MAS NMR spectrum of $TMBA_2[Ir_6(^{13}CO)_{15}]$ recorded at 68.7 MHz, 25 °C, and at a spinning speed of 5.9 kHz. Spinning sidebands marked with * are associated with the peak at δ = 179.0 ppm, while those marked with # are related to the peak at δ = 184.2 ppm.

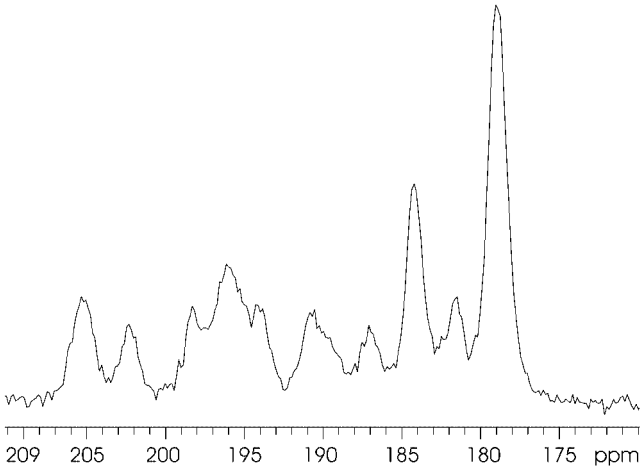

Figure 5. Isotropic region of the solid-state ^{13}C MAS NMR spectrum of $TMBA_2[Ir_6(^{13}CO)_{15}]$ recorded at 68.7 MHz, 25 °C, and at a spinning speed of 5.9 kHz.

The chemical shift tensors (δ_{11}, δ_{22}, and δ_{33}) and the shielding anisotropies ($\Delta\sigma$) associated with the different carbonyl signals (see Table 2) afford further information.

From an accurate spectrum analysis it is possible to observe that the spinning sideband manifolds of the peaks centered at δ = 179.0 and 184.2 ppm are much narrower with respect to the spinning sideband envelopes associated with all other resonances. In particular, the intensities of the first group of the spinning sidebands related to the isotropic peak at δ = 179.0 ppm (marked with * in Figure 4) drastically decrease as well as those associated with the res-

Table 2. ^{13}C chemical shift tensors, shielding anisotropy, and integral values for compound $TMBA_2[Ir_6(CO)_{15}]$. The shielding anisotropy is defined as $\Delta\sigma = \sigma_{33} - (\sigma_{11} + \sigma_{22})/2$ with $\sigma_{11} \leq \sigma_{22} \leq \sigma_{33}$ and $\delta_{ii} = -\sigma_{ii}$.

δ_{iso} [ppm]	δ_{11} [ppm]	δ_{22} [ppm]	δ_{33} [ppm]	$\Delta\sigma$ [ppm]	Integral value
178.9	265.1	165.6	105.9	109.4	2
181.5	303.1	303.1	–61.8	364.9	1
184.2	263.5	172.6	116.5	101.6	1
187.1	359.9	292.4	–90.8	417.0	1
189.5(sh)[a]	364.9[a]	292.5[a]	–87.3[a]	416.0[a]	2
190.5					
193.8[a]					
196.1	358.9[a]	310.7[a]	–81.4[a]	416.2[a]	5
198.3					
202.3	375.1	290.8	–58.9	391.9	1
205.3	389.6	296.3	–69.9	412.8	2

[a] The spinning sideband analysis was performed by considering a single peak, due to high-resonance overlapping. All these resonances are associated to terminal ligands and then a similar anisotropy is expected.

onance at δ = 184.2 ppm (marked with # in Figure 4). Furthermore, we decided to perform the Herzfeld–Berger analysis on the spinning sideband patterns to assert whether terminal and bridging carbonyl ligands give rise to different chemical shift tensor values. The computer simulation of the experimental spinning sideband patterns gave us the tensor and anisotropy values reported in Table 2. By comparing the shielding anisotropies, we can observe that those related to the resonances at δ = 179.0 and 184.2 ppm ($\Delta\sigma$ = 109.4 and 101.6 ppm, respectively) are about 298 ppm lower than the average anisotropy value of the other signals ($\Delta\sigma$ = 404 ppm); since it is well known that the terminal carbonyl ligands have a CSA value of the order of 400 ppm, whereas bridging carbonyl ligands show smaller values,[10,11] we can assert that the resonances at δ = 179.0 and 184.2 ppm are associated with the bridging CO ligands.

The counter-intuitive shifts of the bridging carbonyl ligands to lower frequencies with respect to the terminal ones prompted us to try to rationalize by quantum mechanical calculations the observed spectroscopic data and to take advantage of DFT calculations for a full understanding of the system.

Computational Results

The geometry of $[Ir_6(CO)_{15}]^{2-}$ has been fully optimized by means of the Jaguar program at the B3LYP/LACV3P**++ level, which resulted in a molecular geometry very close to D_3 symmetry, even if no symmetry constrains have been imposed. The geometry (Figure 6) shows three types of carbonyl ligands: two groups of terminal ligands each composed of six carbonyl ligands and a single group of three μ_2-bridging carbonyl ligands. The first type of terminal carbonyl ligands points in between the other two μ_1-carbonyl ligands placed on the adjacent Ir atom (t1 in Figure 6), whereas the other group of six terminal carbonyl ligands (type t2, not labelled in Figure 6) are pointing towards each other. The ^{13}C NMR chemical shifts calculated at this level by the GIAO method employed by Jaguar are intuitively in agreement with the common chemical experience that predicts bridging CO ligands as being less shielded than terminal ones, but do not correlate with the experimental data, resulting in a complete reversal of the order of the assignment of the resonances (Table 3). Methods that can calculate chemical shifts of main group elements are routinely implemented in most standard quantum chemical packages, but the calculation of NMR shielding constants is particularly challenging in $[Ir_6(CO)_{15}]^{2-}$ because relativistic effects are important even for lighter elements if these elements are bound to heavier metals.[12,13] In these atoms the spin-orbit (SO) coupling induces a non-negligible effect. The calculation of NMR parameters, that take into account the SO coupling, has shown an improved agreement with experimentally determined parameters over previous scalar-relativistic calculations for iodo compounds,[14] mercury halides,[13] and for the ^{13}C NMR shifts of 5d transition metal carbonyl complexes.[15] This prompted us to investigate the SO contributions taking advantage of the ADF package.

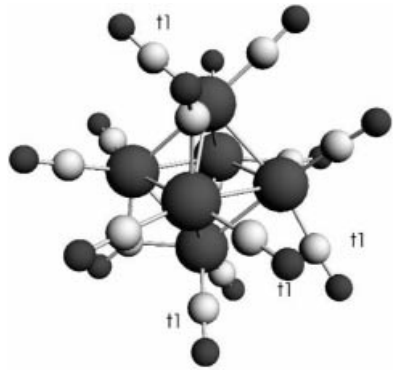

Figure 6. Optimized structure of $[Ir_6(CO)_{15}]^{2-}$, with labels on axial and equatorial terminal carbonyl ligands.

Table 3. Experimental (solution) and calculated[a] ^{13}C NMR parameters (ppm) of $[Ir_6(CO)_{15}]^{2-}$. Paramagnetic (σ^{para}), diamagnetic (σ^{dia}), and relativistic spin-orbit (σ^{SO}) contributions to the values of the absolute isotropic shieldings.

	Exp.	GIAO Jaguar B3LYP/LACV3P**++	GIAO ADF spin-orbit (and scalar) BP-ZORA/TZ2P			
		δ^{iso}	δ^{iso}	σ^{para}	σ^{dia}	σ^{SO}
μ_2-CO	175.2	228.4	187.7 (212.4)	–274.3 (–272.6)	242.7 (242.8)	26.6
μ_1-CO t1	191.2	211.1	198.2 (199.8)	–274.1 (–273.6)	256.4 (256.4)	2.3
μ_1-CO t2	201.1	211.1	203.0 (199.2)	–274.0 (–273.7)	257.1 (257.1)	–3.4

[a] The values are the mean of 3 (μ_2) or 6 (μ_1 t1 and μ_1 t2) carbonyl ligands that are nonequivalent because we do not impose the symmetry during calculations. Standard deviations are typically 0.1 ppm and in any case below 0.3 ppm.

The geometry optimized using the ADF program with the BP-ZORA/TZ2P method is almost identical to that obtained by Jaguar at the B3LYP/LACV3P**++ level. The results of the ZORA spin-orbit (SO) coupling method reproduce the spectroscopic data of the carbon atoms (Tables 3 and 4). A close inspection of the contributions to the values of the absolute isotropic shielding reveals that the paramagnetic part (σ^{para}) has almost the same contribution for all three types of carbonyl ligands. The lower contribution of the diamagnetic part (σ^{dia}) for the bridging μ_2-CO ligands moves the calculated ^{13}C chemical shift to higher values, but a much stronger correction of 26.6 ppm with the opposite sign comes from the relativistic spin-orbit part of the shielding (σ^{SO}). In the case of $[Ir_6(CO)_{15}]^{2-}$, σ^{SO} accounts for almost all the observed trend in the chemical shifts. The calculation of ^{13}C NMR parameters performed with the scalar BP-ZORA/TZ2P method does not differ substantially from those obtained previously by the Jaguar method (Table 3), pointing out the importance of the SO contribution. This appears to be a case in which the combination of spin-orbit coupling and magnetic field mixes spin triplet states into the ground state, inducing a spin density that then interacts with the nuclei of the carbonylmetal via the Fermi-contact term, as already outlined in the literature.[14,15]

Table 4. Calculated chemical shift tensors (δ_{11}, δ_{22}, δ_{33}) and shielding anisotropy ($\Delta\sigma$) for $[Ir_6(CO)_{15}]^{2-}$ with ADF at spin-orbit BP-ZORA/TZ2P level.

δ_{iso} [ppm]	δ_{11} [ppm]	δ_{22} [ppm]	δ_{33} [ppm]	$\Delta\sigma$ [ppm]	Integral value
187.7	247.9	209.2	106.0	122.6	3
198.2	334.0	317.6	–57.2	383.0	6
203.0	345.9	329.3	–66.4	404.0	6

Conclusions

In this paper we have finally solved the NMR assignment of the CO resonances of $TMBA_2[Ir_6(^{13}CO)_{15}]$ by using a complementary solid-state NMR and computational approach. VT solution NMR studies on a ^{13}C-enriched sample of $TMBA_2[Ir_6(^{13}CO)_{15}]$ have shown a fluxionality in the behavior of the CO ligands around the metal cluster. Three sets of carbonyl ligands (two terminal and one bridging) have been found in the cluster giving rise to three peaks in the ^{13}C NMR solution spectrum at low temperatures. An unusually low-frequency chemical shift for the bridging carbonyl ligand has been observed at 173 K when the CO ligands are almost frozen. Solid-state NMR spinning sideband analysis has given further proof to the right assignment of the bridging carbonyl resonance. Indeed, their signals are associated with a much lower $\Delta\sigma$ than the terminal ligands. This confirms the reliability of solid-state NMR spectroscopy as a bridging technique between crystal structure analysis and solution NMR spectroscopy.

Moreover, we demonstrate by means of ADF with the BP-ZORA/TZ2P method that the low-frequency shift in the bridging carbonyl chemical shift has a significant relativistic spin-orbit contribution that cannot be neglected in a proper assignment of the ^{13}C resonances. Therefore, care should also be taken in the evaluation of NMR parameters for lighter elements, in particular when they are bonded to third-row transition metal atoms. The spin-orbit two-component relativistic protocol has been successfully adopted in DFT calculations to evaluate the NMR shielding constants of carbon atoms directly bonded to Ir nuclei. A satisfactory agreement between the calculated and experimental NMR spectroscopic data has been obtained.

Experimental Section

General

All operations were carried out under N_2 using Schlenk tube techniques. Tetrahydrofuran was distilled from Na/naphthalene; all other analytical-grade solvents were degassed and stored under N_2. $[Ir(CO)_4]^-$,[16] $[Ir_4(CO)_{12}]$,[17] $[Ir_6(CO)_{15}]^{2-}$,[18] and $[Ir_6(CO)_{16}]$[19] were prepared according to the published methods; IR spectra were recorded with a Bruker Vector 22 FT-IR spectrophotometer, using 0.1 mm CaF_2 cells previously purged with N_2.

Sample Preparation

It has been proved that $[Ir_6(CO)_{15}]^{2-}$ and the closely related neutral cluster $Ir_6(CO)_{16}$ do not exchange their coordinated CO ligands with gaseous ^{13}CO and hence they cannot be conveniently enriched for ^{13}C NMR studies. Therefore, in order to obtain a ^{13}CO enriched sample of both clusters, we had to follow particular synthetic routes, shown in Scheme 1.

$Ir_4(CO)_{12}$ is the key compound for the preparation of the two hexanuclear clusters. However, its direct ^{13}CO enrichment is impossible owing to its insolubility in all common organic solvents; therefore, a suitable precursor is necessary which can directly exchange with ^{13}CO on the one hand, and on the other hand can be easily transformed back into $Ir_4(CO)_{12}$. This compound is $[Ir_4(CO)_{11}(COOMe)]^-$; in fact it can be obtained by treatment of the parent cluster with sodium methoxide in methanol, it gives a fast exchange with ^{13}CO at room temperature and, as already reported,[20] can regenerate $Ir_4(CO)_{12}$ by simple acidification with acetic acid.

The ^{13}CO-enriched samples of $[Ir_4(CO)_{11}(COOMe)]^-$ (ca. 30%) were obtained by direct exchange at room temperature with the 99% ^{13}CO standard, commercially available from Cambridge Isotope Laboratories, by using standard vacuum-line techniques.

The ^{13}C-enriched tetranuclear cluster then reacts with 2 equiv. of $[Ir(CO)_4]^-$ in refluxing THF to give ^{13}C-enriched $[Ir_6(CO)_{15}]^{2-}$, which can be isolated as a brown reddish powder by precipitation with an aqueous solution of $[(CH_3)_3N(CH_2C_6H_5)]Cl$ or converted into $Ir_6(^{13}CO)_{16}$ by acidification under ^{13}CO (0.051 g, 0.032 mmol, 30% yield).

In a typical preparation, $Ir_4(CO)_{12}$ (1.500 g, 1.359 mmol) was suspended in 60 mL of dry methanol in a 250-mL Schlenk flask and stirred under ^{12}CO at room temperature; 10.6 mL of a 0.9 M solution of $NaOCH_3$ in dry methanol (molar ratio $Ir_4(CO)_{12}/NaOCH_3$ = 1:7) was added dropwise to the light yellow suspension; after about 5 h, a clear orange-yellow solution was obtained, due to the formation of the $[Ir_4(CO)_{11}(COOCH_3)]^-$ derivative. After removing the ^{12}CO in vacuo, the solution was stirred under ^{13}CO (90% v/v) at room temperature for about 4 h. Then an excess of glacial CH_3COOH was added to the solution causing the immediate pre-

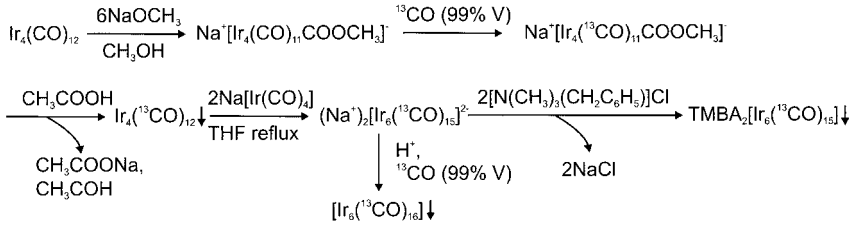

Scheme 1.

cipitation of the light yellow $Ir_4(^{13}CO)_{12}$; the product was filtered, washed several times with water and finally with methanol before being dried in vacuo (1.425 g, 1.291 mmol, 95% yield).

Sodium was added to a suspension of $Ir_4(^{13}CO)_{12}$ (0.429 g, 0.386 mmol) in dry THF (30 mL) and the mixture was vigorously stirred under CO for about 24 h. The FT-IR spectrum of the decanted light yellow liquid showed a typical band of $[Ir(CO)_4]^-$ at 1894 cm^{-1}; the brown mixture was filtered and solid $Ir_4(^{13}CO)_{12}$ (0.437 g, 0.396 mmol) was added to the filtrate. The yellow suspension was heated at the reflux temperature under N_2 for about 24 h; the FT-IR spectrum of the obtained dark red-brown solution showed an intense band at 1984 cm^{-1}, characteristic of the $[Ir_6(^{13}CO)_{15}]^{2-}$ dianion. A solution of $[(CH_3)_3N(CH_2C_6H_5)]Cl$ (0.222 g, 1.193 mmol) in water (60 mL) was then added dropwise to the cluster solution; after removing THF in vacuo, the brown reddish precipitate was collected by filtration, washed with water and finally dried (0.472 g, 0.252 mmol, 64% yield).

NMR Characterization of $Ir_6(^{13}CO)_{16}$ and $TMBA_2[Ir_6(^{13}CO)_{15}]$

Solution NMR Measurements: Solution spectra were recorded with a Bruker Avance 600 spectrometer operating at 150.1 MHz for the ^{13}C nucleus. For the VT experiments the compound $TMBA_2[Ir_6(^{13}CO)_{15}]$ was dissolved in $[D_8]$THF and the temperature was varied between 173 and 298 K.

Solid-State NMR Measurements: Solid-state data were collected with a Jeol GSX 270 spectrometer equipped with a Doty probe operating at 67.8 MHz for ^{13}C and 270 MHz for ^1H. A standard 90° pulse sequence was used with a pulse duration of 2.5 μs corresponding to a 60° pulse. The recycle delay was 250 s to allow the complete recovery of the magnetization after the pulse; 600–2000 transients were sufficient to obtain a good signal/noise ratio. The spectra were recorded at room temperature at different spinning speeds. Cylindrical 5-mm (o.d.) zirconia rotors with sample volumes of 120 μL were employed. For the sample the magic angle was carefully adjusted from the ^{79}Br spectrum of KBr by minimizing the line width of the spinning sideband satellite transitions.

The principal components of the chemical shift tensors were extracted by computer simulation of the spinning sideband patterns obtained at low speed using the HBA program[21] based on the algorithm developed by Herzfeld and Berger.[7] The errors in the evaluation of the chemical shift tensors are less than 4 ppm as evaluated by repetition of the calculation at different spinning speeds. The ^{13}C principal tensor components are reported according to the standard convention[10] where $\delta_{11} \geq \delta_{22} \geq \delta_{33}$ and the shielding anisotropy is defined as $\Delta\sigma = \sigma_{33} - (\sigma_{11}+\sigma_{22})/2$ with $\sigma_{11} \leq \sigma_{22} \leq \sigma_{33}$ and $\delta_{ii} = -\sigma_{ii}$.

Computational Details

The initial geometry of $[Ir_6(CO)_{15}]^{2-}$ was taken from the literature.[9] Calculations were performed either with Jaguar[22] or with ADF2005.1.[23] In Jaguar we adopted the DFT method based on Becke's three-parameter hybrid functional and Lee–Yang–Parr's gradient-corrected correlation functional (B3LYP), with a triple-ζ basis set LACV3P**++,[24] which also includes the outermost core orbitals and effective core potentials (ECPs). The NMR properties were calculated by the GIAO method used by Jaguar.[25] In the geometry optimization carried out with ADF we used the scalar relativistic two-component zero-order regular approximation (ZORA) method,[26] which requires a specially optimized basis set.[27] The default ZORA doubly polarized triple-ζ (TZ2P) basis set was used. The inner shells were represented by the frozen core approximation (1s for C, O and 1s–4d for Ir were kept frozen). We adopted the generalized gradient approximation (CGA) with Becke (exchange) and Perdew (correlation) gradient corrections (BP). The calculations of the NMR parameters were performed by the ADF NMR property module by means of the scalar and the spin-orbit ZORA methods.[28] In the SO coupling method, which takes into account the interactions between the electron magnetic moments and the magnetic field generated by their own orbital motion, the U1K BEST option was used.[23] The absolute isotropic constant shielding values (σ) for ^{13}C of TMS, used as a reference, were calculated from the optimized structures of TMS with Jaguar (σ^{ref} = 184.02 ppm) and with ADF [σ^{ref}(SO) = 182.71 ppm, σ^{ref}(scalar) = 182.61 ppm], with the methods and basis sets described above. The ^{13}C chemical shift values of the carbonyl ligands were therefore calculated as $\delta = \sigma^{ref} - \sigma^{calcd}$.

[1] B. E. Mann, B. F. Taylor, *^{13}C NMR Data for Organometallic Compounds* (Eds.: P. M. Maitlis, F. G. A. Stone, R. West), Academic Press, London, **1981**, and references cited therein.
[2] a) M. J. McGlinchey, *Can. J. Chem.* **2001**, *79*, 1295–1309; b) L. J. Farrugia, A. L. Gillon, D. Braga, F. Grepioni, *Organometallics* **1999**, *18*, 5022–5033.
[3] L. Malatesta, G. Caglio, M. Angoletta, *J. Chem. Soc. C* **1970**, 532–533.
[4] L. Garlaschelli, M. C. Malatesta, S. Martinengo, F. Demartin, M. Manassero, M. Sansoni, *J. Chem. Soc., Dalton Trans.* **1986**, 777–782.
[5] L. Garlaschelli, S. Martinengo, P. L. Bellon, F. Demartin, M. Manassero, M. Y. Chiang, C. Y. Wei, R. Bau, *J. Am. Chem. Soc.* **1984**, *106*, 6664–6667.
[6] B. T. Heaton, A. D. C. Towl, P. Chini, A. Fumagalli, D. J. A. McCaffrey, S. Martinengo, *J. Chem. Soc., Chem. Commun.* **1975**, 523–524.
[7] J. Herzfeld, A. E. Berger, *J. Chem. Phys.* **1980**, *73*, 6021–6030.
[8] T. H. Walter, L. Reven, E. Oldfield, *J. Phys. Chem.* **1989**, *93*, 1320–1326.
[9] F. Demartin, M. Manassero, M. Sansoni, L. Garlaschelli, S. Martinengo, F. Canziani, *J. Chem. Soc., Chem. Commun.* **1980**, 903–904.
[10] G. E. Hawkes, K. D. Sales, S. Aime, R. Gobetto, L.-Y. Lian, *Inorg. Chem.* **1991**, *30*, 1489–1493.
[11] a) E. Oldfield, L. Reven, *Inorg. Chem.* **1992**, *31*, 243–252; b) S. Aime, W. Dastrù, R. Gobetto, G. E. Hawkes, in *Advanced Application of NMR to Organometallic Chemistry* (Eds.: M. Gielen, R. Willem, B. Wrackmeyer), Wiley, Chichester, **1996**.
[12] T. Ziegler, J. Autschbach, *Chem. Rev.* **2005**, *105*, 2695–2722.

[13] M. Kaupp, M. Bühl, V. G. Malkin, *Calculation of NMR and EPR Parameters. Theory and Applications*, Wiley-VCH, Weinheim, **2004**.
[14] M. Kaupp, O. L. Malkina, V. G. Malkin, P. Pyykkö, *Chem. Eur. J.* **1998**, *4*, 118–126.
[15] S. K. Wolff, T. Ziegler, *J. Chem. Phys.* **1998**, *109*, 895–905.
[16] L. Garlaschelli, R. Della Pergola, S. Martinengo, *Inorg. Synth.* **1990**, *28*, 211–215.
[17] F. P. Pruchnik, K. Wajda-Hermanowicz, M. Koralewicz, *J. Organomet. Chem.* **1990**, *384*, 381–383.
[18] M. Angoletta, L. Malatesta, G. Caglio, *J. Organomet. Chem.* **1975**, *94*, 99–106.
[19] R. E. Stevens, P. C. C. Liu, W. L. Gladfelter, *J. Organomet. Chem.* **1985**, *287*, 133–143.
[20] L. Garlaschelli, S. Martinengo, P. Chini, F. Canziani, R. Bau, *J. Organomet. Chem.* **1981**, *213*, 379–388.
[21] K. Eichele, R. E. Wasylishen, *HBA 1.5*, Dalhousie University, Halifax, Nova Scotia.
[22] *Jaguar*, version 6.5, Schrödinger LLC, New York, NY, **2005**.
[23] a) G. te Velde, F. M. Bickelhaupt, S. J. A. van Gisbergen, C. Fonseca Guerra, E. J. Baerends, J. G. Snijders, T. Ziegler, *J. Comput. Chem.* **2001**, *22*, 931–967; b) C. Fonseca Guerra, J. G. Snijders, G. te Velde, E. J. Baerends, *Theor. Chem. Acc.* **1998**, *99*, 391–403; c) ADF2005.01, SCM, Theoretical Chemistry, Vrije Universiteit, Amsterdam, The Netherlands, http://www.scm.com.
[24] The basis set LACVP has been developed at the Los Alamos National Laboratories (see: P. J. Hay, W. R. Wadt, *J. Chem. Phys.* **1985**, *82*, 270–283, 284–298, 299–310). The LACV3P basis set is a triple-zeta contraction of the LACVP basis set developed and tested at Schrödinger, Inc. Lighter elements (i.e. C and O in this case) employ the 6-311G basis set.
[25] Y. Cao, M. D. Beachy, D. A. Braden, L. A. Morrill, M. N. Ringnalda, R. A. Friesner, *J. Chem. Phys.* **2005**, *122*, art. no. 224116.
[26] F. Jansen, *Introduction to Computational Chemistry*, Wiley, Chichester, **1999**.
[27] a) E. van Lenthe, E. J. Baerends, J. G. Snijders, *J. Chem. Phys.* **1993**, *99*, 4597–4610; b) E. van Lenthe, E. J. Baerends, J. G. Snijders, *J. Chem. Phys.* **1994**, *101*, 9783–9792; c) E. van Lenthe, A. E. Ehlers, E. J. Baerends, *J. Chem. Phys.* **1999**, *110*, 8943–8953.
[28] a) G. Schreckenbach, T. Ziegler, *J. Phys. Chem.* **1995**, *99*, 606–611; b) G. Schreckenbach, T. Ziegler, *Int. J. Quantum Chem.* **1997**, *61*, 899–918; c) S. K. Wolff, T. Ziegler, E. van Lenthe, E. J. Baerends, *J. Chem. Phys.* **1999**, *110*, 7689–7698; d) J. Autschbach, T. Ziegler, *J. Chem. Phys.* **2000**, *113*, 936–947; e) J. Autschbach, T. Ziegler, *J. Chem. Phys.* **2000**, *113*, 9410–9418.
Received: November 6, 2006
Published Online: March 28, 2007

